

## MODELLING OFF-ROAD TIRE BEHAVIOUR AND ANALYSING THE MULTI-PASS EFFECT ON VEHICLE DYNAMICS: A COMPREHENSIVE STUDY

---

Amartya Sharma\*  
Dr. Rohit Sharma\*\*

### ABSTRACT

*Off-road activities play a crucial role across various industries, and the intricate interaction between tires and terrain significantly impacts vehicle performance. This research paper focuses on Partially based on observation and experience, an off-road tire designed for various terrains model that combines study of multiple scholars to accurately predict key tire characteristics in scenarios of off road terrain. These characteristics include Traction force exerted on a vehicle's hitch, rotational force that propels the vehicle, sideways force experienced during movement, the effect of tire slip and sinkage, and the repeated traversing of a route behaviour, model's extended to encompass the Essential characteristics of a tyre operating on soil which is soft in nature within unified framework. The approach is extensively discussed, highlighting the vigour and weaknesses of diverse deployment. The research accounts both flexible and rigid tyres, examining the longitudinal/lateral dynamics. Advantage of semi-empirical model lies in its computational efficiency, making it suitable simulations of vehicle dynamics in real-time. Interestingly, current vehicle dynamics codes are found to inadequately address operations on off road, in which the interaction of tyre terrain dominates performance of vehicle. The research focuses on specific twosoil types: and terrain(loose) and firmer moist clay. results achieved demonstrate, model accurately predicts lateral/longitudinal forces, while also giving reliable estimates of slip-sinkage behaviour and sensitivity of tyre parameter. In summary, this research explores a Model of an off-road tire based on empirical observations and analysis, consolidating work of multiple scholars to effectively capture tire behaviour in off-road conditions. The findings emphasize the significance of the tire-terrain interaction and its impact on vehicle performance, highlighting the need for improved representation in dynamics codes of current vehicle.*

**Keywords:** Off-Road Tyre, Tire-Terrain Interaction, Vehicle Performance, Semi-Empirical Tire Model, Soft Soil, Longitudinal and Lateral Dynamics.

---

### Introduction

Operating vehicles on unpaved surfaces is a significant area of interest in various fields such as Military operations, agricultural activities, construction projects, exploration endeavors, recreational pursuits, and mining operations. Interaction between tyres and terrain plays a crucial role in determining the vehicle's mobility and dynamics.

Over the past few decades, mathematical models have been developed [14,15,16,17] To anticipate and elucidate the flexible characteristics of both the tire and the terrain. However, none of the

---

\* B.Tech(ME) + M.Tech(AME) - Integrated, Amity School of Engineering and Technology, Amity University, Noida, U.P., India.

\*\* Amity School of Engineering and Technology, Amity University, Noida, U.P., India.

existing approaches, except for the model proposed by Harnisch et al [2]., encompass all The attributes of a tire functioning on rough or unimproved terrain in a single design. An effective tire model(off road) for simulations must capable of predicting traction, torque, slip-sinkage, and multi-pass effects. Researchers have employed quadruple approaches: Experimental trials, observational studies, partially empirical approaches, and finite element observation each with its own merits and demerits. testing(experimental) involves direct analysis in the field but is limited to specific testing conditions, making it challenging to evaluate. The empirical method relies on measured indexes such as the cone index and Index of manoeuvrability derived from vehicle characteristics In semi-empirical techniques, strength of soil parameters are determined through experiments, & performance of traction is predetermined utilising computation to indicate distribution of stress. Gross traction derived from the relation between soil slip and shear stress displacement. However, deformed tire's geometry needs to be assumed in these calculations. Theoretical models utilize finite element algorithms and, in some cases, discrete element modelling for the soil and finite element modelling for the tire. These models provide a 3D description however needs significant computation resources, making them not quite suitable for simulation in real-time simulations. We now possess theoretical frameworks that heavily depend on algorithms of finite elements to obtain solutions. Certain scholars [18,19,20] have even made efforts to represent soil using discrete element (DE) models and tires using finite element (FE) models. the soil is typically portrayed as a material with properties of perfect plasticity, elasto-plasticity, or visco-plasticity, in FE applications,, while the tire is represented as a visco-elastic material. These models offer comprehensive three-dimensional representations, but their implementation requires significant computational resources and are not suitable for real-time simulations [21,22,23].

#### **Assumption for Tire Model**

While a considerable amount of research has been dedicated to improving tire mobility and traction, there has been a lack of investigation into the combined behaviour of deformable tires on deformable soils in terms of both cornering and traction. Previous studies have predominantly focused on modelling tread deformation while disregarding carcass deformation when examining overall tire deformation. Despite the limited existing literature on this specific topic, our study aims to identify relevant prior work that aligns with our objectives.

In our presented model in this study, we consider both flexible and rigid tires. wheel(rigid) serves as an initial approximation for a flexible tyre. If the stiffened terrain is considerably less than overall stiffness of tyre, the flexible tire can be estimated as a rigid, while simplifying evaluation to a great extent.

- **Grechenko Slip Drift and Slip Model**

The Slip/Drift Model (SDM), proposed by Grechenko, is a tire model specifically designed to simulate tire performance on low sinkage off-road terrains. The central component of SDM gradient of deformation, that is mathematically represented by equation binomic:

$$u = j / x = f (Fu / Fz) - \text{(eq-2.1)}$$

In this equation, the variable "u" is defined as "j/x = f(Fu/Fz)". The term "Fu/Fz" represents the ratio between the applied force and the force required to induce slip in the tread block. On the other hand, "j" represents the slip vector, indicating the direction and magnitude of tire slip. The equation expresses the relationship between these variables and their influence on tire deformation within the SDM.

Grechenko also introduces an additional constraint equation that must be satisfied when using the model. This equation, denoted as:

$$(1-s)F_x \tan(\alpha) - F_y = 0 - \text{(eq-2.2)}$$

relates the coefficient of friction to the deformation gradient within the model. It establishes a connection between the longitudinal force (F<sub>x</sub>) and lateral force (F<sub>y</sub>), slip ratio (s), & tire angle of slip (α). By incorporating this equation into the model, the coefficient of friction can be accurately determined based on the given deformation gradient. This equation provides valuable insights into the relationship between tire deformation and the resulting frictional forces experienced during tire operation. Most existing tire models utilised in off-road vehicle simulations tend to neglect the influence of significant rut formation and the importance of sinkage in determining tractive forces. This approach fails to account for the effects of sinkage on lateral bulldozing and compaction resistance, leading to a lack of accuracy and effectiveness in these models when used as multi-purpose off-road vehicle simulators. Recognising the limitations of such approaches, there is a need to develop tire models that incorporate sinkage effects to

provide a more comprehensive and realistic analysis of off-road vehicle dynamics. By considering sinkage as a crucial factor, these enhanced models can better capture the complex interactions between the tire and the terrain, ultimately improving the accuracy and reliability of off-road vehicle simulations in various scenarios.

- **Modified Tyre Model**

To determine the vertical stress working on tire, pressure-sinkage relationship created by Bekker was utilised.

Bekker's empirical equation of pressure-sinkage is widely utilised in mechanics of soil and vehicle engineering(off road) to predict vehicle performance on deformable terrain. The equation, relates the applied pressure (P) to the sinkage depth (Z) and is formulated as follows:

$$Z = (C * P^n) / (1 + C * d * P^{(n+1)}) - \text{(eq - 2.3)}$$

In this equation, Z represents the sinkage depth, P denotes the applied pressure, and d is the diameter on patch of contact between the tyre& soil. empirical constants C and n vary relying on type of soil and conditions. This equation serves as a valuable tool for estimating tire sinkage on deformable soils, which is crucial for determining tractive forces and overall vehicle performance. However, it should be noted that if a tire remains rigid throughout the simulation, the tire structure cannot relax, leading to inaccurate estimations of the forces exerted by the soil. Additionally, the incorporation of combined slip behaviour is achieved through an empirical saturation function, lacking a comprehensive understanding underlying physical mechanisms responsible for generating tractive forces.

- **Rigid and Flexible Tire**

If pressure distribution along the contact patch of a tire operating on deformable soil remains below the stiffness of the inflated carcass, the tire can be treated as a rigid wheel. In this case, the effective radius (Reff) of the tire remains constant and equal to undeformed (Ru) radius. However, if the pressure within the tire's inflated carcass surpasses the limit undergoes deformation, requiring an approach that is different i.e:Reff = Ru

The situation becomes highly intricate as both the terrain and tyre exhibit elastic characteristics. To address this, equation to compute the deformed shape of tyre are proposed in existing research.

$$R_{eff} = \begin{cases} R_u - R_u \left(1 - \frac{1 - \frac{\delta}{R_u}}{\cos(\theta)}\right) & \text{if } \theta_r < \theta \leq \theta_f \\ R_u - R_u \left(1 - \frac{1 - \frac{\delta}{R_u}}{\cos(\theta_f)}\right) e^{-\beta \left(\sqrt{1+\zeta^2+\zeta}\right)(\theta-\theta_f)} & \text{if } \theta_f < \theta \leq \pi \\ R_u - R_u \left(1 - \frac{1 - \frac{\delta}{R_u}}{\cos(2\pi+\theta_r)}\right) e^{\beta \left(\sqrt{1+\zeta^2-\zeta}\right)(\theta-(2\pi+\theta_r))} & \text{if } \pi < \theta \leq 2\pi + \theta_r \end{cases} \quad \text{(eq - 2.4)}$$

The parameters f and b, which are associated with the, inflation pressure, tire's stiffness, angular velocity, damping, size, and construction, are obtained through experimental means [1]. Harnisch et al. model [2] employs a bigger circle(substitute) to represent the characteristics of a tire that is elastic. While this concept is initially proposed from Bekker, its implementation was hindered by computational complexity. This approach involves substituting a bigger radius in calculation of the patch of contact, resulting to a flatter region of contact that mimics deflected tire's shape.

The flat section between hf and hr rotates counterclockwise when the tire encounters deformable soil, [3,4]. This rotation influences the sinkage amount and is determined by the Sliding, vertical force, and air pressure inside the tire. Supposing the tire's maximum bending or flexing corresponds to unit of stress(max), the flat section rotation can equal to angle hm. To achieve implementation that is flexible, the value of hm can be determined using the following calculation. In this equation, pi0 represents the inflation pressure is nominal, Fz0 corresponds to The point at which the overall rigidity of the tire's carcass is exceeded by the applied load., and c0f and c1f are two empirical parameters now adapted for flexible conditions.

$$\theta_m = \left( \frac{p_i F_z}{p_{i0} F_{z0}} c_{0f} + c_{1f} |s_d| \right) \theta_e \quad \text{(eq - 2.5)}$$

### Experiment Design for Off-road Tire Model

To understand tire behaviour under off-road conditions, it is crucial to accurately determine soil strength as a significant portion of the tractive force relies on soil failure. For this purpose, the use of a ring-shaped shearing device is recommended, although there are differing opinions on its suitability for soil-wheel/soil-tire characterisation. The recommended apparatus serves a dual purpose, allowing for the collection of plate sinkage data for Reece's equation and shear displacement constant data ( $K_x$  and  $K_y$ ). To obtain the necessary data, specific loading conditions must be applied, including a constant vertical load until the soil reaches plastic equilibrium and the addition of surcharge loads to the centre and outside of the annulus. Additionally, for the shear displacement constants, tread pieces should be affixed in different directions, and a combined torsional and vertical load should be applied. These experiments help account for factors such as Moisture content in the soil, pattern of tire tread, and the frictional interaction between soil and rubber, all of which directly affect shear deformation constants and need to be measured experimentally.

The shear ring test is advantageous because it maintains a constant loaded soil area throughout the loading process, eliminating the need for area correction in the obtained data. Wong's approach for bevameter data analysis can be employed to analyze the data derived from this test. Measuring the unit weight of the soil is relatively straightforward and can be accomplished by conducting laboratory tests using a drive cylinder. The standards of ASTM D-1556 & D-2167 outline methods for determining unit weights. To closely replicate field conditions, the apparatus triaxial test is utilized in the configuration of Unconsolidated Undrained (UU) for determining shear strength parameters, instead of The Consolidated Undrained (CU) or Consolidated Drained (CD) conditions configurations. A valuable approach to enhance and validate the off-road tire model involves utilising an experimental setup known as the terramechanics rig. This setup allows scholars to predetermine loading conditions to a tire in specific surface settings, allowing the collection of important information such as moments, and tire conditions and forces. By creating a controlled laboratory environment and incorporating known surface data, such as type of soil, moisture content and density.

### Discussion and Observations

Outcomes are presented in 3 sections: sand(dry), moistclay, and efficiency of traction. In the case of dry sand, which is characterised as a loose and non-cohesive soil, the inflated carcass pressure remains within its limits, resulting in the tire behaving like a rigid wheel. Conversely, moist clay, a soil type which is firmer, demonstrates a stronger relationship between sinkage and pressure, leading to deformation in both the tire and the soil.

The soil properties utilized in this study were obtained from [5] and are provided in a condensed form in Table 1. Ensuring the accurate estimation of these variables is vital to achieve precise outcomes. Table 2 presents the nominal tire properties, while Table 3 summarizes the parameters of tyre for multi-pass calculation and slip sinkage.

| Soil       | k'c  | k'phi    | n    | c(Pa) | O(deg) | kxky(m) | ys(kg/m3) |
|------------|------|----------|------|-------|--------|---------|-----------|
| Dry sand   | 2    | 17658.75 | 0.77 | 130   | 31.11  | 0.038   | 1600      |
| Moist clay | 3.25 | 4600     | 0.99 | 22670 | 22     | 0.015   | 1258      |

Table 1: The undisturbed soil properties utilised in this study were derived from simulations conducted [6,7]

| Ru (m) | w (m) | pi(kPa) | f      | b     | d     |
|--------|-------|---------|--------|-------|-------|
| 0.4    | 0.264 | 241     | 0.0854 | 6.368 | 0.023 |

Table 2: The following table presents the nominal tire properties required for tire geometry calculations. These parameters are specific to the Continental Contitrac SUV P265/70/R17 model and been determined through experimental measurements in [8].

| C0  | c1  | c0f | c1f  | n0  | n1  | k1     | k2     | k3     |
|-----|-----|-----|------|-----|-----|--------|--------|--------|
| 0.4 | 0.2 | 0.2 | 0.05 | 0.8 | 0.6 | 0.1178 | 0.1672 | 0.0348 |

Table 3 Here are the tire parameters utilised for slip-sinkage and multi-pass calculations:

- c0 and c1 values: Obtained from [9].
- c0f and c1f values: Estimated through inspection.
- n0 and n1 values: Taken from [10].

- k1, k2, and k3 values: Extrapolated from [11], as explained in the text.
- Please note that all the aforementioned parameters are dimensionless.

To assess the off-road tire model's performance in pure slip conditions, an analysis comparable to the model used for on-road tires was conducted. The objective was to validate whether the model accurately represents the estimated characteristics of a wheel/tire on off-road surface. By applying quasi-static pure lateral slip inputs ranging from -30 to 30 degrees in 1-deg increments, corresponding forces (lateral) were computed. Results for sandy terrain are depicted in Figure 1, while Figure 2 displays the results for Yolo loam terrain. These figures provide insights into the lateral forces generated by the tire under different slip angles on respective terrains.

#### • Observations- Lateral Slip

For sandy terrain, the tire remained within the limit pressure range, resulting in a rigid wheel regardless of vertical loads ranging from 2000 N - 10000 N. However, an estimated sinkage of approximately 12 cm was observed, which aligns with sinkage data from CRREL for tires of similar size. Figure 1 (a) illustrates a decrease in tire lateral forces as longitudinal slip increases, as expected for sandy terrain. The primary contribution to the sideways force arises from shear forces at the interface, whereas the component of bulldozing force component has minimal impact due to the lack of soil cohesion, despite the tire experiencing significantly higher sinkage compared to Yolo loam terrain. However, an increment in load (vertical), the depth of soil penetration and the impact of the bulldozing force on the overall force contribution escalate, resulting in a steeper increase in lateral force at higher slip angles, as depicted in Figure 1 (b).

For Yolo loam terrain, which exhibits higher cohesion than sandy terrain, the bulldozing force accumulates more rapidly. This leads to lateral forces at non-zero slip ratios exceeding those at zero ratio of slip, particularly at higher angles of slip. The tire remains rigid up to a vertical load on wheel of 6000 N, but on 8000 N and 10000 N, it is modeled as flexible. In Figure 2 (b), a distinct peak at zero slip ratio can be observed as angle of slip increases. Beyond peak, the forces (lateral) stabilize at a constant value. It is assumed the sinkage does not significantly increase with higher vertical wheel loads on such firm soil, mitigating the impact of the sideways bulldozing force on the overall lateral force. Consequently, peak & subsequent lateral forces decay are observed at 8000 N & 10000 N, as displayed in Figure 2

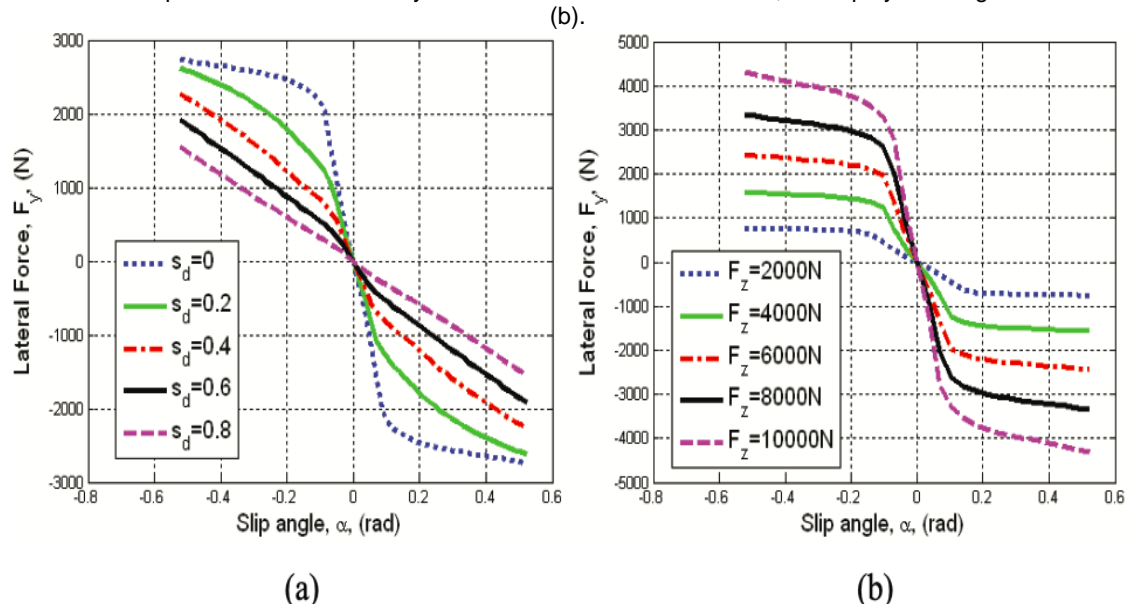


**Figure 1: Shows the lateral forces experienced on sandy terrain. Panel (a) plots the lateral force as a function of angle of slip for different ratios of slip, with a load of reference 6672N. Panel (b) shows the lateral force plotted against angle of slip for different loads (vertical), all at zero ratio of slip**

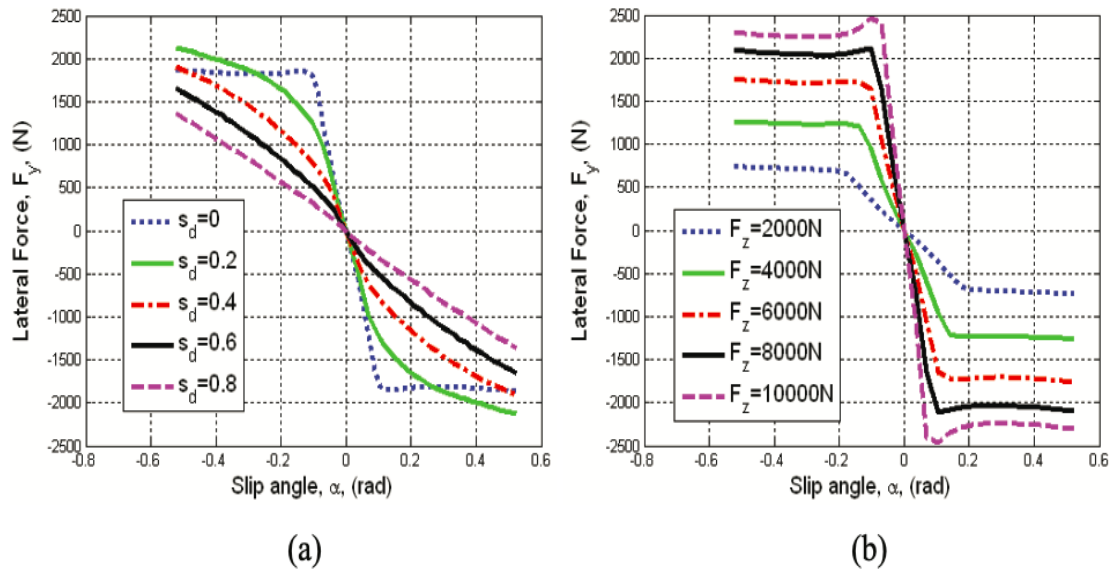


Figure 2: illustrates the lateral forces for moist clay surface, showing (a) the lateral force plotted against angle of slip for different ratios of slip with a load of reference of 6,672 N, and (b) the lateral force plotted against slip angle for different loads(vertical) at zero slip ratio.

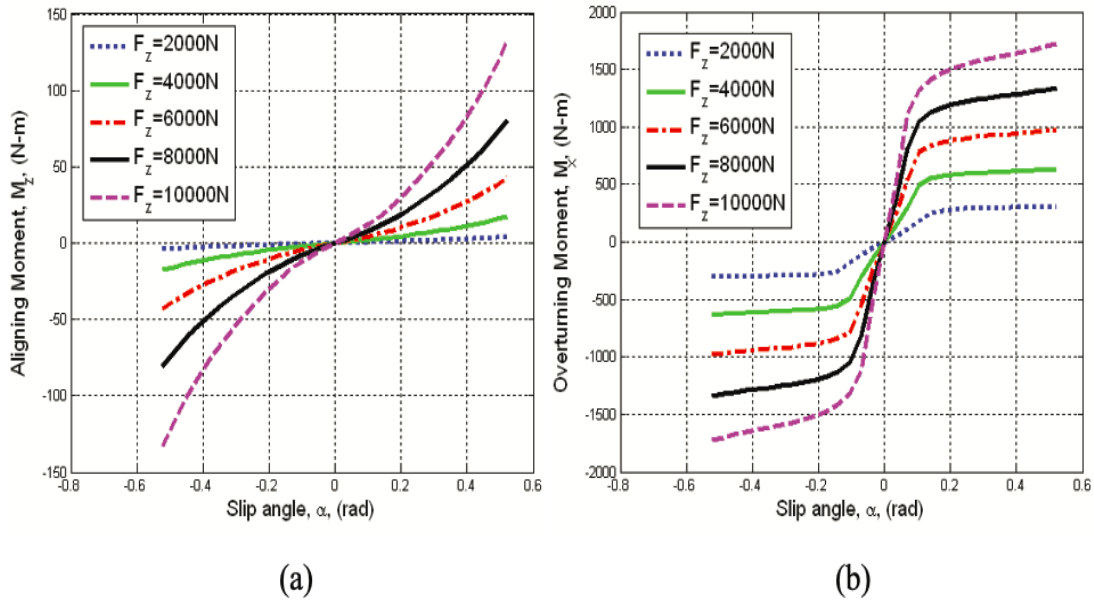
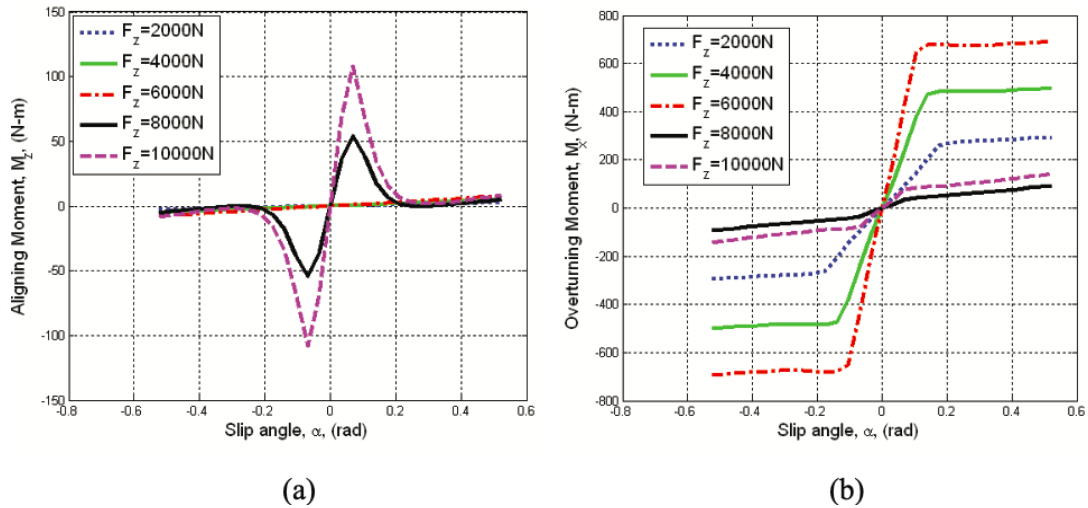


Figure 3: The moments for sand surface are presented. (a) shows the amoment of aligning vs. angle of slip for different vertical loads at zero ratio of slip, while (b) displays the moment of overturning vs. angle of slip for different vertical loads at zero ratio of slip

Figure 1 presents the lateral forces, while Figure 3 illustrates the aligning moment and overturning moment. In contrast to the tire model for tarmac, the aligning moment for the off-road model of tire (Figure 3 (a)) doesn't drop to zero necessarily and turns negative with increasing angle of slip. Increased sinkage contributes to the moment of aligning component due to the force of bulldozing on sand surface. This trend is also observed in the overturning moment (Figure 3



**Figure 4: moist clay surface, the moments,(a) The moment of aligning plotted against the angle of slip for various loads(vertical) at zero slip ratio. (b) The moment of overturning plotted against the angle of slip for various vertical loads at zero ratio of slip.**

Presence of bulldozing force in model explains this phenomenon. However, since the sinkage is not significant in this soil type, the contribution of the force of bulldozing to overall moment is relatively little in comparison to shear forces at contact patch. In Figure 4, the overturning moment follows a similar trend as Figure 4 (b), but the moments for the tyre (flexible) are significantly lower in comparison to ones calculated for a wheel(rigid). This is attributes towards decreased radius resulting from deviation, as well as the reduced sinkage and carcass deflection, which decrease the bulldozing(lateral) component of the total force(lateral).

• **Observation - Longitudinal Slip**

In Figure 5(a), as the slip angle increases, a slight decrease in the force rate is observed at 0.1% slip, indicating that maximum pressure point moves forward as forward slip increases. As the radial stress shift reaches its maximum value, the forces(shear) begin to build up anew and proceeds increasing till they reach saturation. It's important to note that in both Figure 5 (a) and (b), the braking forces are significantly higher than the driving forces due to the sinkage. When the longitudinal force of the tire reaches saturation, it indicates that the wheel is slipping on the sand and can't move ahead without force input from external source at axle.

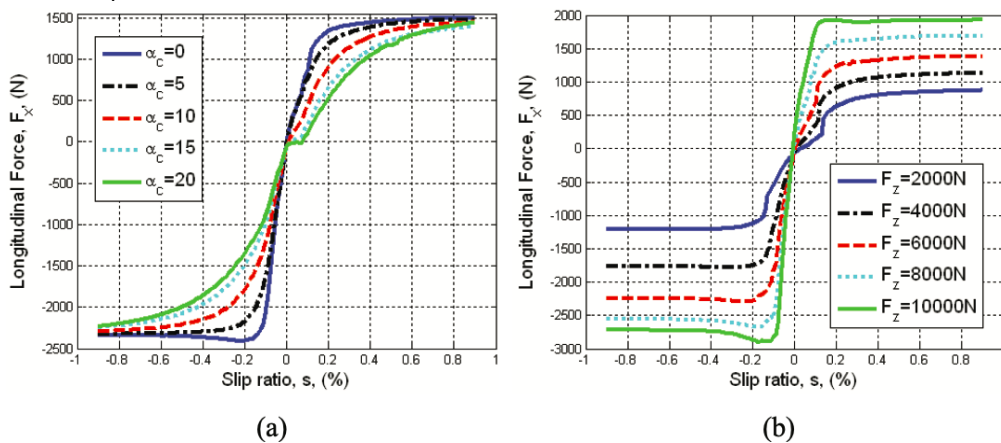


**Figure 5: presents longitudinal forces observed in sandy terrain. In (a), the graph depicts the correlation between force(longitudinal) and ratio of slip for different angles of slip, using a load of reference 6,671 N. Meanwhile, (b) showcases the relationship between force(longitudinal) and ratio of slip for varying loads(vertical) at zero angle of slip.**

Phenomenon has corroborated by data(experimental) gathered[12] [13]. tyre is propelled ahead, slip sinkage and resistance of compaction lead to saturation of force(longitudinal) at + slip, especially in cases of significant sinkage. On the other hand, when the tire is subjected to braking, it digs in the surface, resulting in additional force of stopping through resistance of compaction. According to observation it mirrors driving scenarios in real world.

Figure 6 is a comparative analysis with Figure 5, examining the longitudinal forces in Yolo loam terrain. In Figure 6 (a), the force demonstrates a similar declining pattern as the slip angle increases, albeit with a symmetrical shape that differs from Figure 5 (a). Notably, both figures exhibit a distinct Peak point in the longitudinal force at around 0.11% slip. Conversely, Figure 6 (b) portrays the forces(longitudinal) for various vertical loads, revealing a closer similarity between positive and negative slip compared to Figure 5 (b). The contrasting behavior between these figures can be attributed to Yolo loam having less sinkage than sand, resulting in reduced compaction resistance as factor of limitation for generation of traction. Consequently, the tire's behavior on Yolo loam resembles that of road model of tyre on firmersurface, albeit with the limit of traction being determined by failure of soil at the tire-soil interface. The limit of traction curves in Yolo loam exhibit a smaller area compared to the on-road tire model, while maintaining a relatively conical shape.

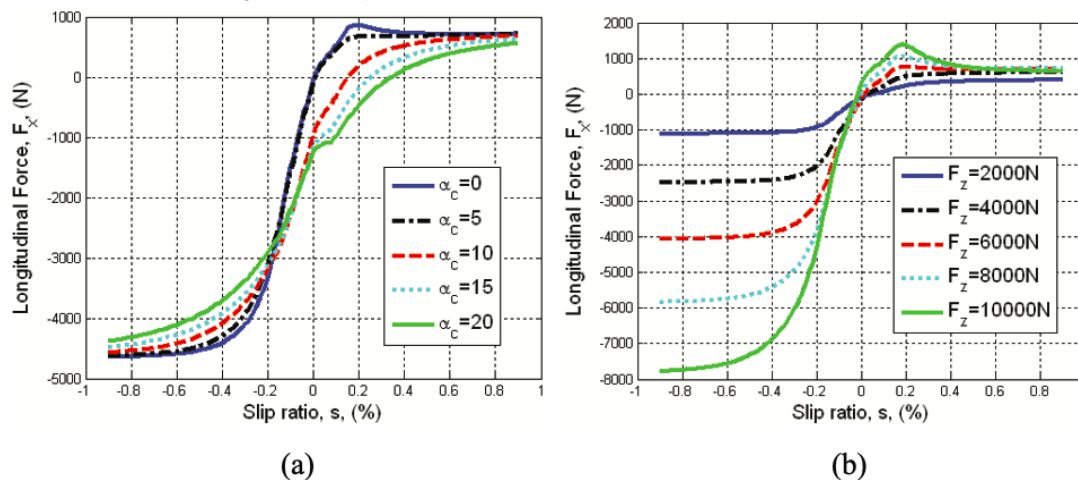


**Figure 6:** presents the longitudinal forces observed in Yolo loam terrain. In Figure 5.8 (a), the plot showcases the correlation between longitudinal force and slip ratio across various slip angles, utilizing a load of reference of 6,671 N. Meanwhile, Figure 5.8 (b) illustrates the connection between force(longitudinal) and slip ratio for different vertical loads at zero angle of slip

- **Low Speed Combined Slip**

Sinkage effects, the model underwent testing for combined slip operation at low speeds, excluding dynamic effects. This involved sweeping the longitudinal slip across a range of -80% to 80% in different angles of slip. Figure 7 showcases the behaviour of combined slip in sandy terrain for varying wheel loads. At a wheel load of 2,000 N, the lateral and longitudinal forces exhibit a traction envelope similar to that of on-road tire models. However, as the wheel load increases, the maximum sinkage (as depicted in Figure 7) also increases, leading to a more significant contribution from compaction and bulldozing forces. In cases where sinkage significantly impacts the total lateral and longitudinal forces, the longitudinal forces at high positive ratios of slip and angles of low slip might exceed envelope of traction, as seen in Figure 7 (c) and (d). Nevertheless, increasing the angle of slip reduces Total shear force produced in either orientation and brings it within the general range. It is important to note that the Moho-Coulomb failure criteria envelope only covers the force components resulting from shear stresses at wheel-soil interface, while The bulldozing and compaction resistance forces have no limits due to limited experimental data determining their limits. These forces are influenced by sinkage, with their impact increasing as sinkage increases.

Figure 8 presents the combined slip forces observed in Yolo loam terrain. Notably, the plot exhibits a symmetrical pattern around the y-axis, which differs from the asymmetry seen in Figure 7. Plots (a), (b), (c), and (d) in Figure 8 share a similar shape, except for a cusp that appears at the point where longitudinal slip equals zero. This occurrence can be attributed to the faster increase of lateral



force compared to longitudinal force at low slip, which is influenced by the soil's higher cohesion. When the soil has greater cohesion, the lateral bulldozing force escalates rapidly with increasing slip angle, contrasting the behavior observed in sandy terrain. However, at a certain point, the lateral force reaches its maximum as the limited bulldozing action can only generate a certain level of thrust at specific slip angles. Figure 9 demonstrates that when the model of tire transitions towards a flexible model of tyre, The greater contact area leads to a reduction in maximum sinkage. This accounts for the consistent magnitude of cusps generated by the lateral bulldozing force, even with an increase in wheel load the lateral displacement of soil remains approximately constant. The behavior of the model in combined slip aligns with the observations of tire movement typically observed in off-road terrain. Given the variations in testing conditions, tire types, and wheel loads employed in this study, these findings should be considered qualitatively.

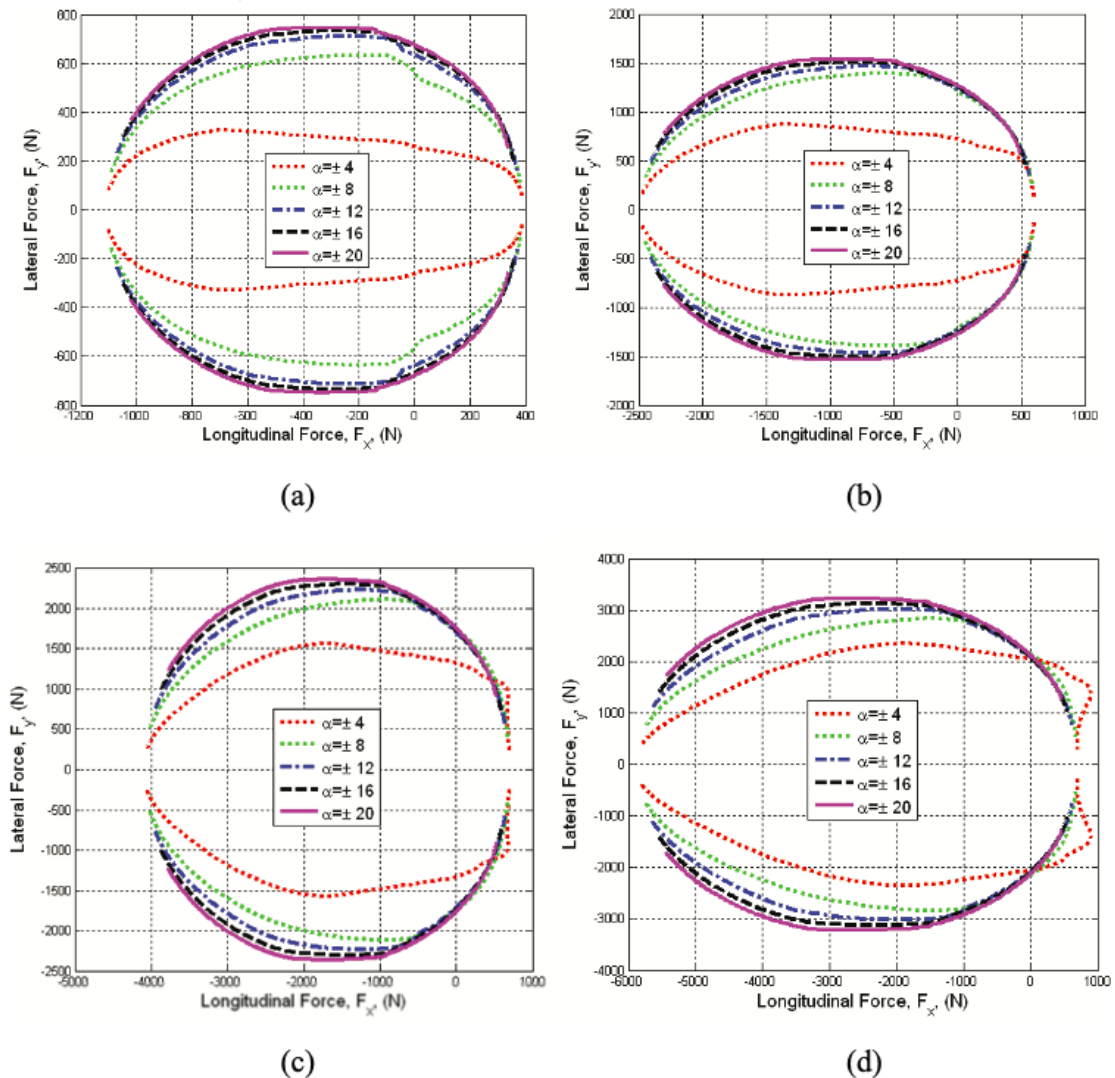


**Figure 7:** showcases the combined slip forces in sandy terrain, presenting different sub-figures for varying vertical tire loads. More specifically, (a) Depicts the forces corresponding to a tire load of 2,000 N, (b) showcases the forces associated with a tire load of 4,000 N, (c) demonstrates the forces observed with a tire load of 6,000 N, and (d) portrays the forces recorded with a tire load of 8,000 N

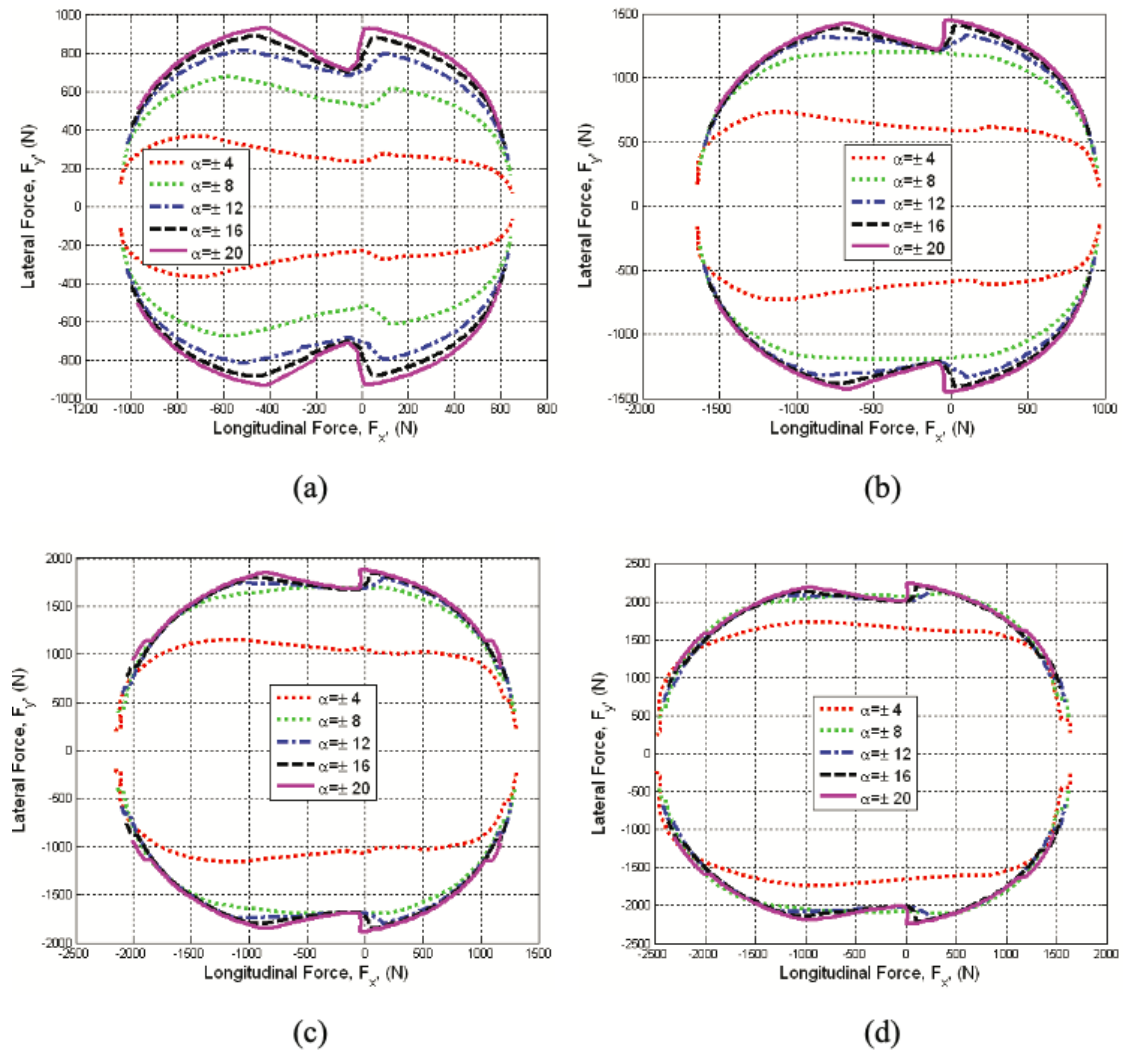


**Figure 8:** Portrays the slip(combined) forces in Yolo loam terrain, presenting subplots (a), (b), (c), and (d) that depict the forces produced by different vertical tire loads of 2,000 N, 4,000 N, 6,000 N, and 8,000 N, respectively

- ### Mobility Map Discussion

Referring to Figure 9, which presents a mobility map illustrating the outcomes obtained for the three different terrains examined. In sandy soils prone to sinkage, The rise in driving force is constrained as the slip ratio increases, while the longitudinal braking force significantly exceeds the driving force. Consequently, when wheel load(vertical) is increased on sandy terrain, the envelope tilts more to the side of braking. Conversely, more resilient soils like Yolo loam, the mobility envelope takes on a shape like cone, indicating a more equitable spread of forces between braking and driving. It is noteworthy conical shape observed in Figure 9 (b) closely resembles a downscaled version of shape depicted in Figure 9 (c) for road tires. Softer soils exhibit heightened braking capabilities due to sinkage, however demonstrate reduced mobility at the front. In contrast, firmer terrain strike a better balance between mobility at the front and braking, although their tractive capabilities remain lower than those experienced in on-road conditions. These findings align well with the typical behaviour observed in off-road tires operating under such circumstances.

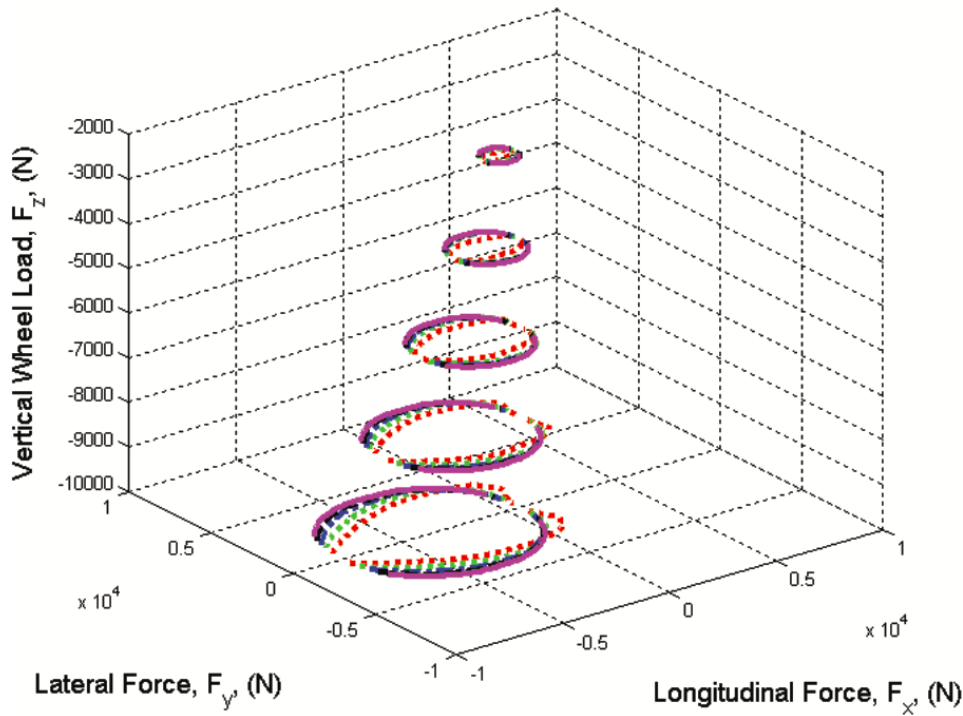
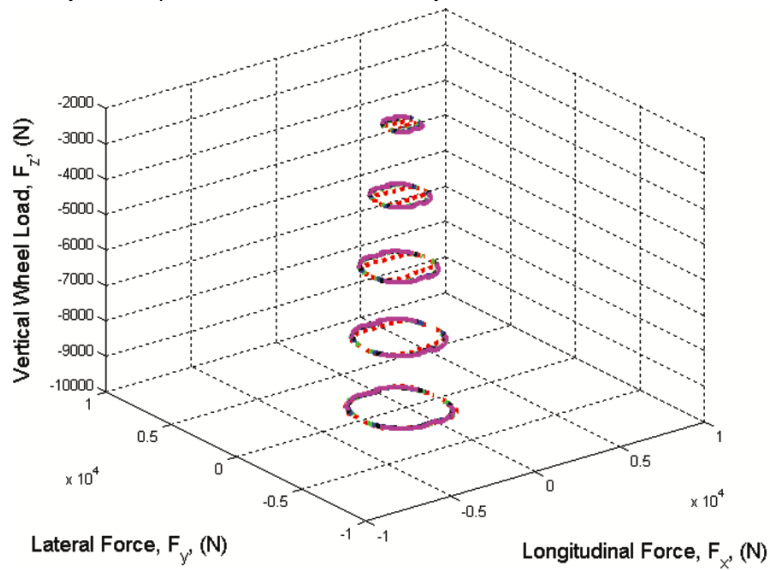
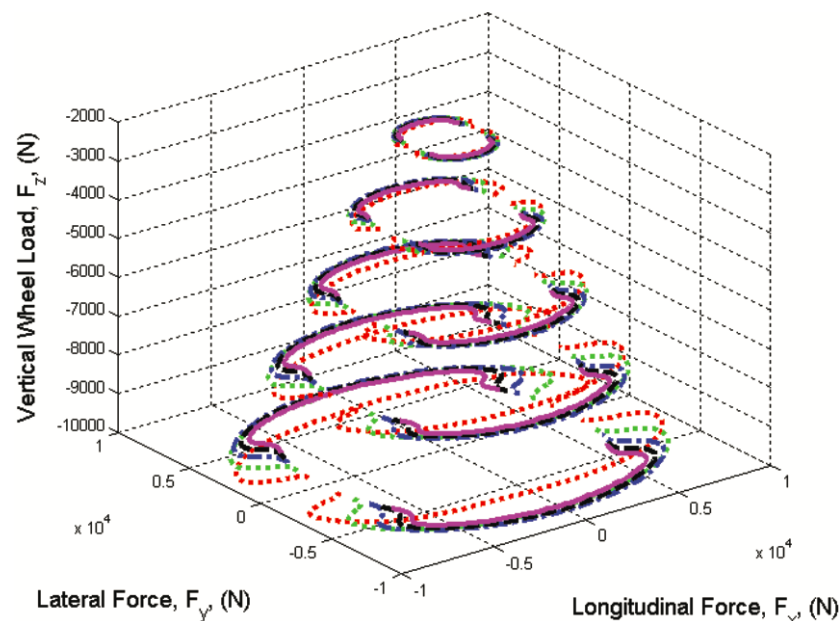


Figure 9 (a): depicts the relationship between the vertical wheel load and the longitudinal and lateral forces of the tyre model on various terrains. map shows results of Sandy terrain.

**Conclusion**

The present chapter provides a summary of the outcomes obtained from the research carried out in this study. The major findings are emphasized, and recommendations are proposed for expanding the scope of this research and enhancing the tire model introduced in this study in the future. The aim of this study was to create a tire model capable of off-road driving for vehicle dynamics simulations. Since the inception of tires on motor vehicles, there has been a continuous drive to improve their design, which has led to increased try to comprehend as mechanised systems.





**Figure 9 (b)(c): depicts the relationship between the vertical wheel load and longitudinal and lateral forces of the tyre model on various terrains. map shows results of Yolo loam terrain and tarmac respectively**

Plasticity theory and mechanical modeling were applied, using theory of center of rotation instantaneous to find the location where max stress(principle) acts on tyre . The tyre model was designed to utilize a mechanical approach, where forces of traction are calculated by integrating the stresses(shear) at the contact interface of tyre use of the flexible tyre for simulate tyre bending is a step forward over methods that are empirical observations on the proper use of this method were integrated into the model, providing a good method to compute interface stresses on tyre after soil failure occurs at the interface. Finally, the tyre model accounted for sinkage effects by including forward compaction resistance and lateral bulldozing resistance when determining traction performance.

#### References

1. Bauer R, Leung W, Barfoot T. Experimental and simulation results of wheel–soil interaction for planetary rovers. In: International conference on intelligent robots and systems, Edmonton, August 2–6, 2005.
2. Harnisch C, Lach B, Jakobs R, Troulis M, Nehls O. A new tyre–soil interaction model for vehicle simulation on deformable ground. *Vehicle Syst Dyn* 2005;43(Supplement):384–94.
3. Freitag DR, Smith ME. Center-line deflection of pneumatic tires moving in dry sand. *J Terramechanics* 1966;3(1):31–46.
4. Karafiath LL, Nowatzki EA. Soil mechanics for off-road vehicle engineering. Clausthal, Germany: Trans Tech Publications.; 1978
5. Wong JY. Terramechanics and off-road vehicle engineering. 2nd ed. UK: Elsevier; 2010.
6. Wong JY, Reece AR. Prediction of rigid wheel performance based on analysis of soil–wheel stresses, part I. Performance of driven rigid wheels. *J Terramechanics* 1967;4(1):81–98.
7. Liang D, Hai-bo G, Zong D, Jian-guo T. Wheel slip-sinkage and its prediction model of lunar rover. *J Cent South Univ Technol* 2010;17:129–35.
8. Chan BJ, Sandu C. Development of an off-road capable tire model for vehicle dynamics simulations, PhD thesis, Virginia Polytechnic Institute and State University, Blacksburg, VA; 2008.
9. Holm IC. Multi-pass behaviour of pneumatic tires. *J Terramechanics* 1969;6(3):47–71.
10. Wong, J. Y., 1980, "Data Processing Methodology In the Characterization of the Mechanical Properties of Terrain," *Journal of Terramechanics*, 17(1), pp. 13-41.
11. Upadhyaya, S. K., Wulfsohn, D. , 1993, "Traction prediction using soil parameters obtained with an instrumented analog device," *Journal of Terramechanics*, 30(2), pp. 85-100.

12. Shmulevich, I., Osetinsky, A., 2003, "Traction performance of a pushed/pulled drive wheel," *Journal of Terramechanics*, 40(1), pp. 33-50
13. Muro, T., O'Brien, J., 2004, *Terramechanics: Land Locomotion Mechanics*, A.A. Balkema, Lisse.
14. Bekker MG. *Off-the-road locomotion; research and development in terramechanics*. Ann Arbor: The University of Michigan Press; 1960
15. Grecenko A. Slip and drift of the wheel with tyre on soft ground. In: *Proceedings of 3rd ISTVS international conference*, vol. II, Essen, Germany; 1969. p. 76–95.
16. Wong JY. *Theory of ground vehicles*. 3rd ed. New York: John Wiley & Sons; 2001.
17. Liang C, Allen RW, Rosenthal TJ, Chrstos J, Nunez P. Tire modeling for off-road vehicle simulation. In: *Proceedings of the 2004 SAE automotive dynamics, stability and controls conference*, Detroit, MI; 2004.
18. Nakashima H, Oida A. Algorithm and implementation of soil-tire contact analysis code based on dynamic finite element method. *J Terramechanics* 2004;41:127–37
19. Zhang R, Li J. Simulation on mechanical behavior of cohesive soil by distinct element method. *J Terramechanics* 2006;43(3):303–16.
20. Koizumi T, Tsujiuchi N, Mori S. Simulation of grouser–soil interaction by using 3-dimensional DEM considering particle roughness. In: *Proceedings of 16th ISTVS international conference*, Turin, Italy; 2008. p. 221–7
21. Shoop S, Kestler K, Haehnel R. Finite element modeling of tires on snow. *Tire Sci Technol* 2006;34(1):2–37.
22. Oida S, Seta E, Heguri H, Kato K. Soil/tire interaction analysis using FEM and FVM. *Tire Sci Technol* 2005;33(1):38–62.
23. Shoop S, Darnell I, Kestler K. Analysis of tire models for rolling on a deformable substrate. *Tire Sci Technol* 2002;30(3):180–97.

#### Nomenclature

- $b$  penetrometer characteristic length
- $b, d, f$  coefficients needed to calculate deflected tire shape
- $c_{soil}$  cohesion
- $c_0, c_1, c_0f, c_1f$  coefficients related to the angle where maximum stress occurs
- $F_{xdrawbar}$  longitudinal force
- $F_y, F_{ybd}, F_{ylateral}$  lateral force, lateral force due to bulldozing lateral force due to shear
- $\gamma_s$  soil density
- angle of internal friction of the soil
- $j_x, j_y$  longitudinal and lateral shear displacement
- $k'$  cohesion related soil parameter
- $k'$  angle internal friction related soil parameter
- $k_x, k_y$  shear deformation modulus in the longitudinal and lateral direction
- $k_1, k_2, k_3$  multi-pass coefficients
- $l'_p$  Projected Contact patch length
- $n$  Bekker sinkage coefficient
- $n_0, n_1$  Bekker slip sinkage coefficient
- $N_c, N_c, N_q$  Terzaghi bearing capacity factors
- $q$  surcharge load
- $R_{eff}, R_u, R_{leffective}$  undeformed, and rolling radius
- $\sigma_n$  normal stress along the contact patch
- $s_d$  slip ratio
- angular coordinate along the contact patch where maximum stress is
- $\theta_e, \theta_{entry}$  and exit angle
- $t$  tangential stress along the contact patch
- $z$  Sinkage
- $w$  width.

